Structures of medium-sized silicon clusters

Kai-Ming Ho*, Alexandre A. Shvartsburg†, Bicai Pan*, Zhong-Yi Lu*, Cai-Zhuang Wang*, Jacob G. Wacker*, James L. Fye† & Martin F. Jarrold†

** Ames Laboratory-USDOE and Department of Physics and Astronomy, Iowa State University, Ames, Iowa 50011, USA*

† Department of Chemistry, Northwestern University, 2145 Sheridan Road, Evanston, Illinois 60208, USA

Silicon is the most important semiconducting material in the microelectronics industry. If current miniaturization trends continue, minimum device features will soon approach the size of atomic clusters. In this size regime, the structure and properties of materials often differ dramatically from those of the bulk. An enormous effort has been devoted to determining the structures of free silicon clusters[1–22]. Although progress has been made for Si_n with $n < 8$, theoretical predictions for larger clusters are contradictory[2–22] and none enjoy any compelling experimental support. Here we report geometries calculated for medium-sized silicon clusters using an unbiased global search with a genetic algorithm. Ion mobilities[23] determined for these geometries by trajectory calculations are in excellent agreement with the values that we measure experimentally. The cluster geometries that we obtain do not correspond to fragments of the bulk. For $n = 12–18$ they are built on a structural motif consisting of a stack of Si_9 tricapped trigonal prisms. For $n \geq 19$, our calculations predict that near-spherical cage structures become the most stable. The transition to these more spherical geometries occurs in the measured mobilities for slightly larger clusters than in the calculations, possibly because of entropic effects.

The structures of small ($n < 8$) silicon clusters have been extensively studied by theoretical methods. Except for $n = 5$, the structures of these clusters have been confirmed by anion photoelectron spectroscopy[24], or by Raman[25] and infrared[26] measurements on matrix-isolated clusters. As the cluster size increases, it becomes much more difficult to find the lowest-energy structure in theoretical studies because the number of possible geometries increases exponentially. Extensive searches have been performed for slightly larger silicon clusters ($n = 8–11$) but some of the conclusions are still the subject of debate[6,7,9,10,20]. For $n > 13$, only geometries constructed following assumed bonding schemes have been presented. None of the structures proposed for $n > 7$ have been experimentally verified. Anion photoelectron spectroscopy and Raman and infrared studies of matrix-isolated clusters have not yet been able to provide ground-state vibrational frequencies for clusters with more than seven atoms. This leaves ion mobility measurements as the only experimental method currently available to provide information about the structures of silicon clusters containing over a dozen atoms. This method has been successfully applied to carbon clusters[27]. Previous mobility measurements[23] for Si_n^+ have only been interpreted qualitatively to indicate that silicon clusters become prolate between $n = 10$ and 23, then for larger clusters a structural transition to a more spherical geometry occurs. Here we take advantage of the recent implementation of a classical trajectory method for evaluating mobilities[28], and perform a quantitative comparison of the measured mobilities with those determined for the calculated geometries.

An unbiased global search for the ground state structures of

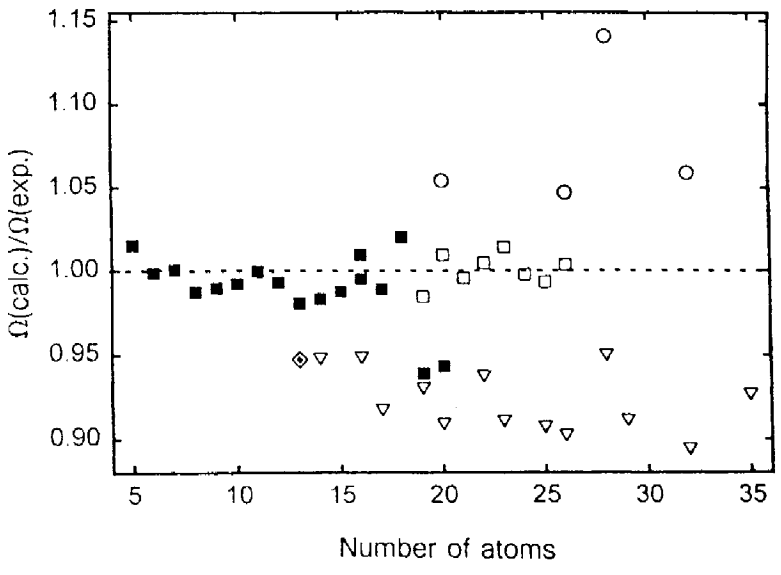

Figure 1 Relative deviations of the collision integrals for proposed silicon cluster geometries from the values measured at 298 K. Empty circles and triangles are for the families of "puckered six-fold rings"[18,19] and "alternating triangles".[20] Filled and empty squares are for our geometries described in the text, and shown in Figs 2 and 3. Icosahedral Si_{13} is shown by a diamond. For $n < 18$, measurements were also performed at 78 K and the relative deviations are similar to those shown here.

silicon clusters with 11–20 atoms was performed by means of a genetic algorithm[29]. This is an optimization strategy based on modelling biological evolution. A population of structures is optimized, and the fittest members selected to 'parent' the next generation through a 'mating' process. Here we operate with a population of 16 clusters with four 'parents'. The 'offspring' clusters of each generation are relaxed by molecular dynamics quenching. The fully relaxed structure is incorporated into the parent population if its energy is below that of its parents, and discarded otherwise. The procedure is continued for at least 600 generations, with multiple ecologies ensuring a truly global search. Initially, the energies are estimated using a new tight-binding potential (C.Z.W. *et al.*, manuscript in preparation) developed to reproduce the results of density functional theory calculations using the local density approximation (LDA). For the promising isomers, LDA was used to evaluate the energies. To check the convergence of the search procedure, a parallel independent search was performed using simulated annealing with a Car-Parrinello LDA technique. For $n \leq 16$, simulated annealing and the genetic algorithm find the same global minima. However, for larger clusters, the energies of structures found by the genetic algorithm are lower. The searches were performed for neutral clusters, but the lowest-energy isomer for each size was fully relaxed as a cation. The changes in the geometries are negligible in all cases.

Ion mobilities were measured using a tandem quadrupole drift-tube apparatus that has previously been described in detail[30]. The clusters were generated by laser vaporization of a silicon rod, entrained in a helium flow, ionized by a 1.1 keV electron beam, mass selected, and injected into a drift tube containing helium buffer gas. Mobilities are measured by injecting a 20–50 μs pulse of cluster ions into the drift tube and recording the arrival time distribution at the detector. Measurements were performed at drift-tube temperatures of 78 and 298 K. The drift-tube buffer gas pressure was 2.5–9.4 torr, the drift voltage was 13.3 V cm^{-1}, and the injection energy was 50 eV. In all cases, the experiments were carried out in the low drift field regime where the mobility is independent of the field.

The reduced mobility of a gas phase ion is inversely proportional to the orientationally averaged collision integral for the ion and buffer gas. Collision integrals for candidate geometries were calculated by propagating classical trajectories in a realistic intermolecular potential[28]. This potential is constructed as a sum of pairwise Si–He interactions plus a charge-induced dipole term. Each pairwise interaction is treated as having the Lennard–Jones form and the charge is assumed to be delocalized over all the atoms. Recent work for carbon clusters[31] has demonstrated that this model is more accurate than previously used approximations. To apply this model here, we first need to determine the elementary Si–He potential. This is accomplished by fitting the temperature dependence of the mobility of a cluster with known geometry. The two largest clusters with experimentally confirmed geometries, Si_6 (D_{4h} tetragonal) and Si_7 (D_{5h} pentagonal bipyramid)[25,26] were used. The only parameters adjusted in the fit are the depth of the potential, ϵ, and the intercept, σ. The values obtained were $\epsilon = 1.35$ meV and $\sigma = 3.50$ Å. Mobilities calculated for the correct Si_n^+ structures should agree with the measurements at both 78 and 298 K to within[27] ~2%. This error margin includes the experimental uncertainty and the estimated uncertainties in both the mobility calculations and the bond lengths and bond angles of the candidate structures.

We have evaluated the mobilities for two isomer families proposed in the literature: the "stacked puckered six-fold rings" of Kaxiras and Jackson[18,19] and the "stacked triangles" of Grossman and Mitas[20]. The results are shown in Fig. 1. The mobilities calculated for both isomer families deviate systematically from the measurements for the prolate isomers: the "stacked six-fold rings" are always too prolate and the "stacked triangles" are not prolate enough. The mobilities calculated for the lowest-energy geometries resulting from our unbiased structural optimization (filled squares in Fig. 1) are within 2% of the measurements for $n \leq 18$. The LDA energies of these geometries are substantially lower than for all previously proposed isomers for $n > 11$.

For $n = 8$ the measured mobilities compare well with those evaluated for the previously accepted lowest-energy geometry[7,8,15]: a C_{2h} distorted bicapped octahedron. In all-electron calculations[7], the C_s distorted tricapped octahedron and C_{2v} distorted tricapped trigonal prism (TTP) are nearly degenerate for $n = 9$, and the T_d tetracapped octahedron and C_{3v} tetracapped trigonal prism are nearly degenerate for $n = 10$. Recently, Chelikowsky and collaborators[6] have found a C_{2v} capped stacked rhombi structure to be the ground state of Si_9. The mobilities calculated for all three Si_9 isomers agree with the measurements. However, the mobility computed for T_d Si_{10} is in significantly worse agreement with the measurements than the C_{3v} geometry, which virtually rules out the T_d geometry. This supports recent calculations[20] affirming the C_{3v} geometry as the ground state for Si_{10}. We can definitely eliminate all non-compact (tetrahedral bonding network) structures and unreconstructed fragments of bulk Si lattice advanced for small silicon clusters[10].

For $n = 11$, we obtain the C_{2v} structure of Rohlfing and Raghavachari[8] as the global minimum. However, the other six isomers considered in ref. 8—except for the two pentacapped octahedrons that are high in energy—have mobilities which also agree with our measured values. The previously accepted structures for $n = 12$ and 13 were a C_{2v} hexacapped trigonal prism[16] and a C_{3v} capped trigonal antiprism[21], respectively. Our calculated geometries, which are shown in Fig. 2, are lower in energy by 0.6 eV for Si_{12} and 0.3 eV for Si_{13}. Unfortunately, for these clusters the old and new

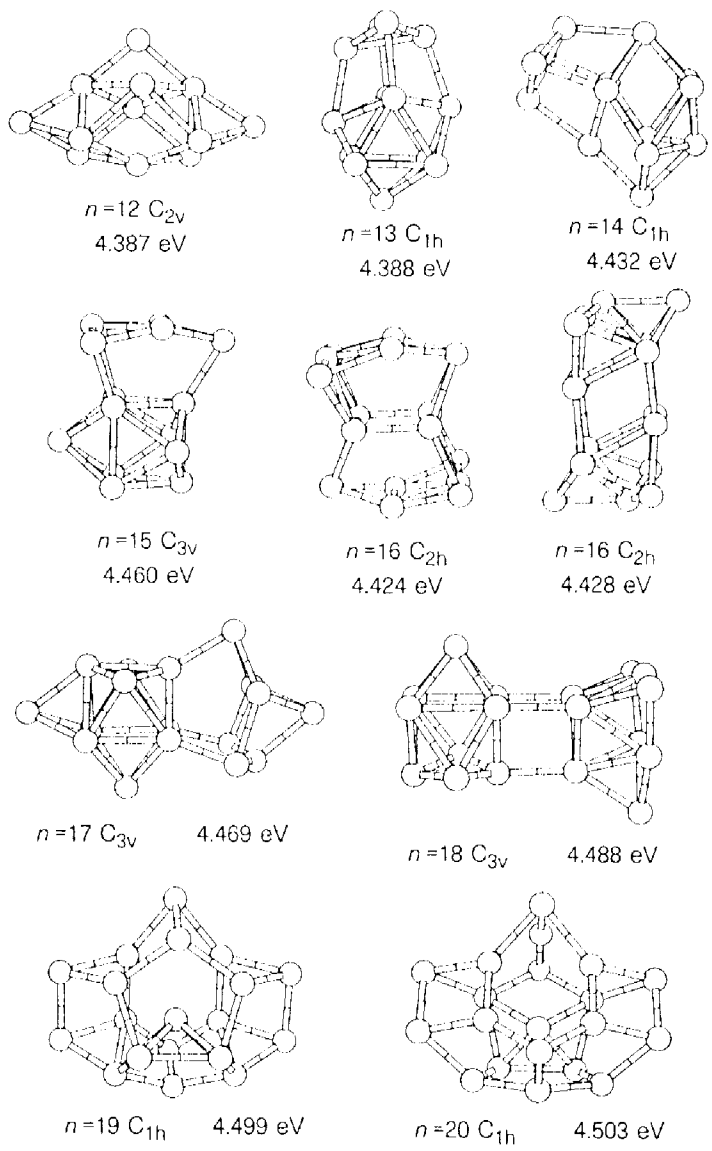

Figure 2 The LDA global minima for the Si_n (n = 12-20) neutrals. Cohesive energies per atom are indicated. The two geometries shown for Si_{16} are essentially degenerate.

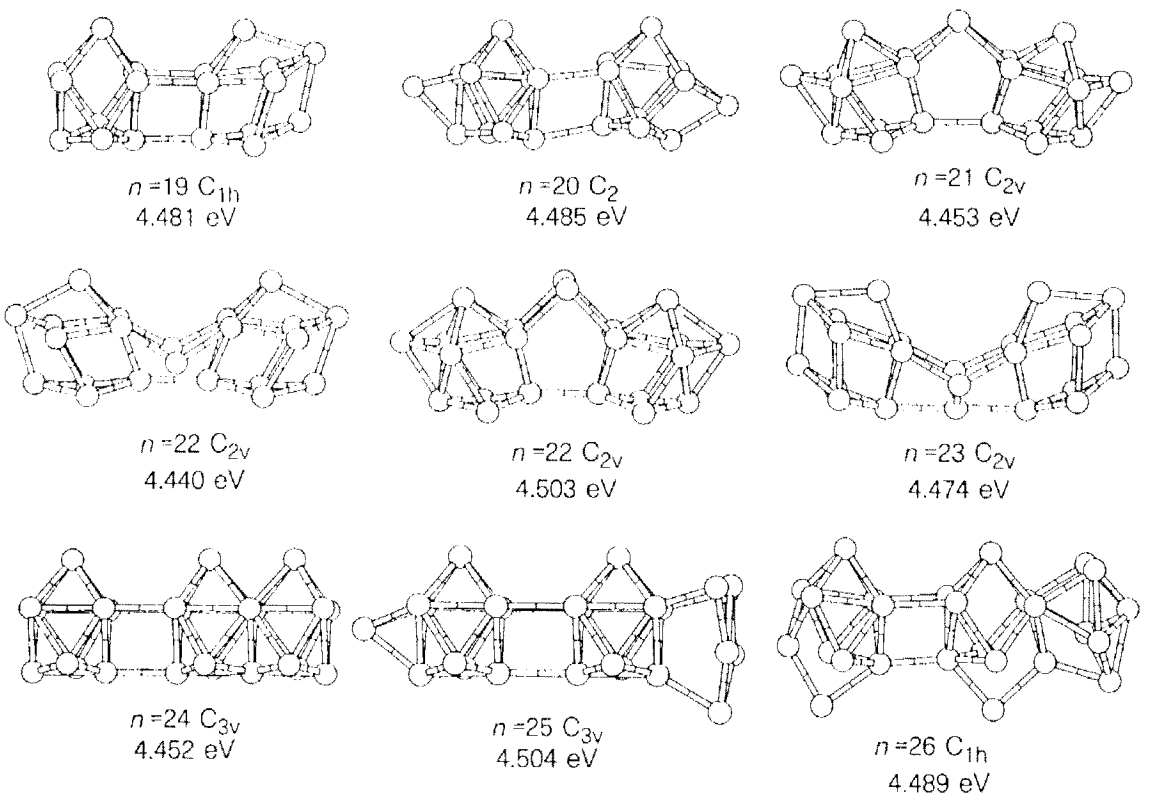

Figure 3 Prolate geometries for $n = 19$–26 constructed by stacking Si_9 TTP subunits. The structures for $n = 19$ and 20 were relaxed, while the others are not necessarily local minima.

structures could not be distinguished experimentally as their mobilities are within 1% of each other. We can, however, exclude icosahedral Si_{13}, the existence of which has been the subject of much debate[4,5,13,14,17,20,21] (see Fig. 1). The mobility becomes really sensitive to geometry for $n \geq 14$. In this size range, our structures are lower in energy than those previously known[20] by 1.2 eV (Si_{14}), 0.9 eV (Si_{16}) and 2.7 eV (Si_{17}), and are the only proposed geometries to have the right mobilities. For $n = 15$ and 16, we have found two structures that are degenerate within the accuracy of the LDA calculation. For $n = 15$, only the C_{3v} structure has a calculated mobility that agrees with the measurements, whereas for $n = 16$ the calculated mobilities of both geometries agree. In the $n < 19$ size range, our geometries can be visualized as stacked Si_9 tricapped trigonal prisms (see Fig. 2) as first conjectured by Jarrold and Constant[23].

Starting from $n = 19$, our computed global minima drastically change from the prolate assemblies of Si_9 subunits to more compact cage-like geometries (Fig. 2). The calculated mobilities for this new family of isomers disagree with the measured values until $n \geq 24$, where they fit the second experimentally observed ("spherical") isomer. So the structural rearrangement shown in Fig. 2 apparently corresponds to the "prolate-to-spherical" transition that begins at $n = 24$ in the experiments[23]. The discrepancy in the point of onset could be due to an entropic effect similar to that found for carbon clusters. For carbon, the fullerene is predicted to be the most stable geometry[32] for a cluster as small as C_{20}^+, but C_{30}^+ is the smallest fullerene observed experimentally[27]. This occurs because at the high temperature required to induce isomerization, the fullerene is not a low-free-energy structure for the smaller clusters. It only becomes competitive[33] around C_{28}. Because the prolate structures are not the lowest-energy isomers for silicon clusters with $n \geq 19$ (according to the LDA calculations), geometries for the prolate isomers that persist in the mobility measurements to larger cluster sizes[23] cannot be obtained using the genetic algorithm. However, these geometries can be built-up by stacking Si_9 TTP prisms following the patterns established for $n < 19$. We have constructed such structures up to $n = 26$ (see Fig. 3). Their mobilities (empty squares in Fig. 1) agree with the measurements, which supports our assignment of all prolate clusters as Si_9 TTP stacks. These structures for $n > 19$ are not necessarily unique, as several geometries with minor variations often differ in mobility by less than 1%, for example two isomers for $n = 22$ in Fig. 3. As these geometries are not the result of a systematic search, it is possible that other, lower-energy structures might also fit the mobilities of the "prolate" family for $n \geq 19$. However, our prolate isomers are lower in energy than any previously proposed[18–20,22] for Si_n, $n = 19$–26, by 1–4 eV. In fact, they are (to our knowledge) the first geometries reported for $n = 17$, 18 and $n = 22$–26 that are energetically stable against spontaneous fission into two smaller clusters.

Received 1 September; accepted 17 December 1997.

1. Pacchioni, G. & Koutecky, J. Silicon and germanium clusters. A theoretical study of their electronic structures and properties. *J. Chem. Phys.* **84,** 3301–3310 (1986).
2. Tomanek, D. & Schluter, M. A. Calculation of magic numbers and the stability of small Si clusters. *Phys. Rev. Lett.* **56,** 1055–1058 (1986).
3. Slee, T., Zhenyang, L. & Mingos, D. M. P. Polyhedral skeletal electron pair theory of bare clusters. 1. Small silicon clusters. *Inorg. Chem.* **28,** 2256–2261 (1989).
4. Chelikowsky, J. R., Glassford, K. M. & Phillips, J. C. Interatomic force fields for silicon microclusters. *Phys. Rev. B* **44,** 1538–1545 (1991).
5. Phillips, J. C. Electron-correlation energies and the structure of Si_{13}. *Phys. Rev. B* **47,** 14132–14135 (1993).
6. Vasiliev, I., Ögüt, S. & Chelikowsky, J. R. *Ab Initio* calculations for the polarizabilities of small semiconductor clusters. *Phys. Rev. Lett.* **78,** 4805–4808 (1997).
7. Raghavachari, K. & Rohlfing, C. M. Bonding and stabilities of small silicon clusters: a theoretical study of Si_7–Si_{10}. *J. Chem. Phys.* **89,** 2219–2234 (1988).
8. Rohlfing, C. M. & Raghavachari, K. A theoretical study of small silicon clusters using an effective core potential. *Chem. Phys. Lett.* **167,** 559–565 (1990).
9. Raghavachari, K. & Rohlfing, C. M. Structures of Si_{10}. Are there conventionally bonded low-energy isomers? *Chem. Phys. Lett.* **198,** 521–525 (1992).
10. Messmer, R. P. & Patterson, C. H. Long bonds in silicon clusters: a failure of conventional Møller-Plesset perturbation theory? *Chem. Phys. Lett.* **192,** 277–282 (1992).
11. Mistriotis, A. D., Froudakis, G. E., Vendras, P. & Flytzanis, N. Model potential for silicon clusters and surfaces. *Phys. Rev. B* **47,** 10648–10653 (1993).
12. Jug, K. & Krack, M. Consistent parameterization of semiempirical MO methods. *Int. J. Quant. Chem.* **44,** 517–531 (1992).
13. Gu, B., Li, Z. & Zhu, J. Electrical structure of small icosahedral silicon clusters. *J. Phys.: Condens. Matter* **5,** 5255–5260 (1993).
14. Gong, X. G., Zheng, Q. Q. & He, Y. Z. Structural properties of silicon clusters: an empirical potential study. *J. Phys.: Condens. Matter* **7,** 577–584 (1995).
15. Menon, M. & Subbaswamy, K. Nonorthogonal tight-binding molecular-dynamics scheme for silicon with improved transferability. *Phys. Rev. B* **55,** 9231–9234 (1996).
16. Ramakrishna, M. V. & Bahel, A. Combined tight-binding and density functional molecular dynamics investigation of Si_{12} cluster structure. *J. Chem. Phys.* **104,** 9833–9840 (1996).
17. Wales, D. J. Electronic structure of small silicon clusters. *Phys. Rev. A* **49,** 2195–2198 (1994).
18. Kaxiras, E. & Jackson, K. Shape of small silicon clusters. *Phys. Rev. Lett.* **71,** 727–730 (1993); Structural models for intermediate-sized Si clusters. *Z. Phys. D* **26,** 346–348 (1993).
19. Pederson, M. R., Jackson, K., Porezag, D. V., Hajnal, Z. & Frauenheim, T. Vibrational signatures for low-energy intermediate-sized Si clusters. *Phys. Rev. B* **54,** 2863–2867 (1996).
20. Grossman, J. C. & Mitas, L. Quantum Monte Carlo determination of electronic and structural properties of Si_n clusters. *Phys. Rev. Lett.* **74,** 1323–1326 (1995); Family of low-energy elongated Si_n ($n \leq 50$) clusters. *Phys. Rev. B* **52,** 16735–16738 (1995).
21. Rothlisberger, U., Andreoni, W. & Giannozzi, P. Thirteen-atom clusters: equilibrium geometries, structural transformations, and trends in Na, Mg, Al, and Si. *J. Chem. Phys.* **96,** 1248–1256 (1992).
22. Song, J., Ulloa, S. E. & Drabold, D. A. Soliton-induced lattice relaxation and the electronic and vibrational spectra of silicon clusters. *Phys. Rev. B* **53,** 8042–8051 (1996).
23. Jarrold, M. F. & Constant, V. A. Silicon cluster ions: evidence for a structural transition. *Phys. Rev. Lett.* **67,** 2994–2997 (1991).
24. Arnold, C. C. & Neumark, D. M. Study of Si_4 and Si_4^- using threshold photodetachment (ZEKE) spectroscopy. *J. Chem. Phys.* **99,** 3353–3362 (1993).
25. Honea, E. C. *et al.* Raman spectra of size-selected silicon clusters and comparison with calculated structures. *Nature* **366,** 42–44 (1993).
26. Li, S., Van Zee, R. J., Weltner Jr, W. & Raghavachari, K. Si_3-Si_7. Experimental and theoretical infrared spectra. *Chem. Phys. Lett.* **243,** 275–280 (1995).
27. Von Helden, G., Hsu, M. T., Gotts, N. G. & Bowers, M. T. Carbon cluster cations with up to 84 atoms: structures, formation mechanism, and reactivity. *J. Phys. Chem.* **97,** 8182–8192 (1993).

28. Mesleh, M. F., Hunter, J. M., Shvartsburg, A. A., Schatz, G. C. & Jarrold, M. F. Structural information from ion mobility measurements: effects of the long-range potential. *J. Phys. Chem.* **100**, 16082–16086 (1996).
29. Deaven, D. M. & Ho, K. M. Molecular geometry optimization with a genetic algorithm. *Phys. Rev. Lett.* **75**, 288–291 (1995).
30. Jarrold, M. F. Drift tube studies of atomic clusters. *J. Phys. Chem.* **99**, 11–21 (1995).
31. Shvartsburg, A. A., Hudgins, R. R., Dugourd, Ph. & Jarrold, M. F. Structural elucidation of fullerene dimers using high-resolution ion mobility measurements and trajectory calculation simulations. *J. Phys. Chem. A* **101**, 1684–1688 (1997).
32. Bylaska, E. J., Taylor, P. R., Kawai, R. & Weare, J. H. LDA predictions of C_{20} isomerizations: neutral and charged species. *J. Phys. Chem.* **100**, 6966–6972 (1996).
33. Martin, J. M. L. C_{28}: the smallest stable fullerene? *Chem. Phys. Lett.* **255**, 1–6 (1996).

Acknowledgements. We thank J. Chelikowsky, D. Drabold, G. Froudakis, J. Grossman, K. Jackson, K. Jug, M. Krack, U. Landman, H. Mayne, M. Menon, L. Mitas, L. Munro, K. Raghavachari, C. Rohlfing, K. Subbaswamy and D. Wales for providing us with their optimized silicon cluster geometries and for discussions; we also thank R. Hudgins for assistance with the experimental work. This research was supported by the NSF, the US Army Research Office, the Office of Basic Energy Sciences, the High Performance Computing and Communications initiative (including a grant of computer time at the National Energy Research Supercomputing Center), and Ames Laboratory operated for the US DOE by Iowa State University.

Correspondence and requests for materials should be addressed to M.F.J. (e-mail: mfj@chem.nwu.edu).